



Calhoun: The NPS Institutional Archive DSpace Repository

Theses and Dissertations

1. Thesis and Dissertation Collection, all items

1999-12

Numerical study for Global Detection of cracks embedded in beams

Lipsey, Stephen A.

Monterey, California: Naval Postgraduate School

<http://hdl.handle.net/10945/13449>

Downloaded from NPS Archive: Calhoun



<http://www.nps.edu/library>

Calhoun is the Naval Postgraduate School's public access digital repository for research materials and institutional publications created by the NPS community.

Calhoun is named for Professor of Mathematics Guy K. Calhoun, NPS's first appointed -- and published -- scholarly author.

**Dudley Knox Library / Naval Postgraduate School
411 Dyer Road / 1 University Circle
Monterey, California USA 93943**

NAVAL POSTGRADUATE SCHOOL
Monterey, California



THESIS

**NUMERICAL STUDY FOR GLOBAL DETECTION
OF CRACKS EMBEDDED IN BEAMS**

by

Stephen A. Lipsey

December 1999

Thesis Advisor:

Young W. Kwon

Approved for public release; distribution is unlimited.

REPORT DOCUMENTATION PAGE

Form Approved
OMB No. 0704-0188

Public reporting burden for this collection of information is estimated to average 1 hour per response, including the time for reviewing instruction, searching existing data sources, gathering and maintaining the data needed, and completing and reviewing the collection of information. Send comments regarding this burden estimate or any other aspect of this collection of information, including suggestions for reducing this burden, to Washington Headquarters Services, Directorate for Information Operations and Reports, 1215 Jefferson Davis Highway, Suite 1204, Arlington, VA 22202-4302, and to the Office of Management and Budget, Paperwork Reduction Project (0704-0188) Washington DC 20503.

1. AGENCY USE ONLY (Leave blank)	2. REPORT DATE December 1999	3. REPORT TYPE AND DATES COVERED Master's Thesis
4. TITLE AND SUBTITLE NUMERICAL STUDY FOR GLOBAL DETECTION OF CRACKS EMBEDDED IN BEAMS		5. FUNDING NUMBERS
6. AUTHOR(S) Lipsey, Stephen A.		
7. PERFORMING ORGANIZATION NAME(S) AND ADDRESS(ES) Naval Postgraduate School Monterey, CA 93943-5000		8. PERFORMING ORGANIZATION REPORT NUMBER
9. SPONSORING / MONITORING AGENCY NAME(S) AND ADDRESS(ES)		10. SPONSORING / MONITORING AGENCY REPORT NUMBER
11. SUPPLEMENTARY NOTES The views expressed in this thesis are those of the author and do not reflect the official policy or position of the Department of Defense or the U.S. Government.		
12a. DISTRIBUTION / AVAILABILITY STATEMENT Approved for public release; distribution unlimited.		12b. DISTRIBUTION CODE
13. ABSTRACT Damage reduces the flexural stiffness of a structure, thereby altering its dynamic response. Considerable effort has been put into obtaining a correlation between the changes in modal parameters and the location and amount of the damage within the structure. Most numerical research employed elements with reduced beam stiffness to simulate damage in the beam. This approach to damage simulation neglects the non-linear effect that a crack has on the structural dynamic response. In the present study, finite element modeling techniques are utilized to directly represent an embedded crack. The results of the dynamic analysis of the present model are then compared to the results of the dynamic analysis of the reduced modulus finite element model. Different modal parameters are investigated to determine the most sensitive indicator of damage and its location. Nonlinear effects, such as crack closure and opening, of an embedded crack on the structural dynamic response were also studied from transient nonlinear analysis. The modeling technique is then applied to sandwich composite beams with simulated delamination to investigate damage detection techniques through the use of damping caused by frictional dissipation of energy on the crack surface.		
14. SUBJECT TERMS Finite Element Analysis, Modal Analysis, Non-destructive damage detection, and Composite Materials		15. NUMBER OF PAGES 64
		16. PRICE CODE
17. SECURITY CLASSIFICATION OF REPORT Unclassified	18. SECURITY CLASSIFICATION OF THIS PAGE Unclassified	19. SECURITY CLASSIFICATION OF ABSTRACT Unclassified
		20. LIMITATION OF ABSTRACT UL

NSN 7540-01-280-5500
239-18

Standard Form 298 (Rev. 2-89)
Prescribed by ANSI Std.

THIS PAGE INTENTIONALLY LEFT BLANK

Approved for public release; distribution is unlimited.

**NUMERICAL STUDY FOR GLOBAL DETECTION OF CRACKS
EMBEDDED IN BEAMS**

Stephen A. Lipsey
Lieutenant, United States Navy
B.S.M.E., United States Naval Academy, 1994

Submitted in partial fulfillment of the
requirements for the degree of

MASTER OF SCIENCE IN MECHANICAL ENGINEERING

from the

NAVAL POSTGRADUATE SCHOOL
December 1999

Author:

Stephen A. Lipsey

Approved by:

Young W. Kwon, Thesis Advisor

Terry R. McNelley, Chairman
Department of Mechanical Engineering

THIS PAGE INTENTIONALLY LEFT BLANK

ABSTRACT

Damage reduces the flexural stiffness of a structure, thereby altering its dynamic response. Considerable effort has been put into obtaining a correlation between the changes in modal parameters and the location and amount of the damage within the structure. Most numerical research employed elements with reduced beam stiffness to simulate damage in the beam. This approach to damage simulation neglects the non-linear effect that a crack has on the structural dynamic response. In the present study, finite element modeling techniques are utilized to directly represent an embedded crack. The results of the dynamic analysis of the present model are then compared to the results of the dynamic analysis of the reduced modulus finite element model. Different modal parameters are investigated to determine the most sensitive indicator of damage and its location. Nonlinear effects, such as crack closure and opening, of an embedded crack on the structural dynamic response were also studied from transient nonlinear analysis. The modeling technique is then applied to sandwich composite beams with simulated delamination to investigate damage detection techniques through the use of damping caused by frictional dissipation of energy on the crack surface.

THIS PAGE INTENTIONALLY LEFT BLANK

TABLE OF CONTENTS

I. INTRODUCTION	1
II. LITERATURE REVIEW.....	5
III. FINITE ELEMENT MODELING AND ANALYSIS.....	9
IV. FINITE ELEMENT MODEL COMPARISON.....	15
A. MODEL.....	15
B. RESULTS.....	17
V. LINEAR DYNAMIC ANALYSIS	21
A. MODEL.....	21
B. RESULTS.....	22
VI. NONLINEAR DYNAMIC ANALYSIS.....	37
A. INTRODUCTION.....	37
B. ANALYSIS AND RESULTS.....	37
VII. CONCLUSIONS AND RECOMMENDATION.....	43
LIST OF REFERENCES.....	47
BIBLIOGRAPHY.....	49
INITIAL DISTRIBUTION LIST.....	51

THIS PAGE INTENTIONALLY LEFT BLANK

LIST OF FIGURES

Figure 1. Four-Noded Beam Element with Six Dof's.....	9
Figure 2. Finite Element Mesh for Beam with Reduced Modulus in Damaged Section	16
Figure 3. Finite Element Mesh for Beam with Embedded Crack	16
Figure 4. Finite Element Mesh for Composite Beam with Crack	22
Figure 5. First Modal Displacement of Embedded Crack Model	24
Figure 6. Second Modal Displacement of Embedded Crack Model	25
Figure 7. Third Modal Displacement of Embedded Crack Model	26
Figure 8. Fourth Modal Displacement of Embedded Crack Model.....	27
Figure 9. Fifth Modal Displacement of Embedded Crack Model.....	28
Figure 10. First Curvature Mode of Embedded Crack Model..	29
Figure 11. Second Curvature Mode of Embedded Crack Model.	30
Figure 12. Third Curvature Mode of Embedded Crack Model..	31
Figure 13. Fourth Curvature Mode of Embedded Crack Model.	32
Figure 14. Fifth Curvature Mode of Embedded Crack Model..	33
Figure 15. Modal Sensitivity to Damage Plot.....	35
Figure 16. Transient Analysis Model.....	38
Figure 17. Crack Opening vs Time.....	41
Figure 18. Relative Axial Displacement of Crack Surface vs Time.....	41

THIS PAGE INTENTIONALLY LEFT BLANK

x

LIST OF TABLES

Table 1.	Frequencies for Embedded Crack Model.....	18
Table 2.	Frequencies for 7e-7% Reduced Modulus Model....	18
Table 3.	Frequencies for 25% Reduced Modulus Model.....	18
Table 4.	Frequencies for 94% reduced Modulus Model.....	19
Table 5.	Maximum Percent Change.....	23
Table 6.	Damping Ratio According to Friction Coefficient	39
Table 7.	Damping Ratio According to Crack Size.....	39
Table 8.	Damping Ratio According to Crack Location.....	40

THIS PAGE INTENTIONALLY LEFT BLANK

I. INTRODUCTION

The ability to monitor a structure and detect damage at the earliest possible stage is a very important asset in all realms of civil, mechanical, and aerospace engineering disciplines. Many existing methods of damage detection use various non-destructive techniques such as visual, acoustic emission, ultrasounds, magnetic fields, radiographs, eddy-currents, C-scan, and vibration thermographs. Almost all of these methods are inherently localized and require prior knowledge of the possible damage location in order to avoid wasting time during useless data collection. Using these methods for large scale or global areas can be quite expensive as well as require large amounts of labor and time. Therefore, an alternate approach that incorporates the evaluation of a single global parameter or combination of global parameters to detect, localize, and monitor damage would greatly enhance the safety and efficient maintenance of structures.

More recent work in the area of global damage detection techniques has involved the use of relative shifts or changes in the modal parameters. Modal parameters such as modal frequency, modal damping, and mode shapes are a

function of the mass-inertia and elastic properties of the structure. Therefore, the dynamic response of a system can be a sensitive indicator of change in the integrity of the system's elastic structure. Damage in any form reduces the local flexural stiffness in the vicinity of the damage. Reduced stiffness leads to a decrease in modal frequencies and an increase modal damping coefficients as well as changes in the corresponding mode shapes.

Damage can affect the dynamic response of a structure either linearly or nonlinearly. Changes in the dynamic response of the structure subject to linear damage can be related to uniform changes in the geometry or the material properties of the structure. However, in most cases damage is predominantly in the form of micro-scale or macro-scale cracks or voids. Such cracks or voids behave nonlinearly under dynamic excitation as in the case where embedded cracks subsequently open and close. In some nonlinear cases, the global effect of damage on the dynamic response of the structure can be considered to be small and local in nature. In such cases, the damage can be modeled linearly. However, in the case where the nonlinear local behavior significantly affects the global structural response, the damage can no longer be modeled linearly.

Most of the previous research has concentrated on linearized modeling of damage. In these linear eigenvalue analyses using the finite element method, using either reduced material properties or reduced geometric dimensions within the damaged section simulated damage. The focus of these studies was aimed at establishing a modal parameter or method of manipulating modal parameters to obtain the highest sensitivity to damage in the structure. However, in linearizing crack damage in this fashion most researchers must reduce the flexural stiffness in the damaged elements in large amounts to produce relatively small changes in the modal parameters. Little thought has been centered on the effects of linearization of local crack response or in the direct representation of an embedded local crack in a finite element model.

One of the objectives of this study is to evaluate the previous modeling technique, which smeared a crack into a reduced material or geometric properties. To this end, the present study includes an embedded crack modeled directly instead of smearing the crack through reduced material or geometric properties. Linear eigenvalue analysis was performed for this model to compare the present modeling technique with previous smearing techniques used in damage

detection research. In this study, the crack behavior was linearized.

The second objective was to investigate the modal parameter or combination of modal parameters that was more sensitive to a local embedded crack using the present modeling technique. For example, modal frequency, mode shape displacement, mode shape curvature, etc. were examined for a possible modal parameter, which would provide accurate information regarding the presence of a crack and its location.

The final objective was to examine the local nonlinear behavior (such as crack opening and closure) of a crack using transient nonlinear analysis. The effort was made to evaluate the linear eigenvalue analysis conducted in the first portion of the study. Furthermore, the transient nonlinear analysis was utilized to investigate damage detection and localization through a new modal damping (energy dissipation) parameter.

II. LITERATURE REVIEW

There is quite a large amount of literature generated on global damage detection and localization by use of changes in modal parameters. The majority of literature reviewed for the current research has been focused on damage modeling techniques, the modal parameters being utilized for damage detection and localization, and the level of sensitivity to the presence of damage.

The amount of literature related to damage detection using relative shifts in modal frequencies is quite large. Most results summarize a relatively low sensitivity of frequency shifts to damage and the need for very precise measurements for damage detection. This is mainly due to the reduction in flexural stiffness being local in nature, thereby resulting in modal frequency shifts that are hardly detectable with the current test equipment. Spyros (1990) found a modal frequency shift of less than 5% corresponding to a 50% reduction in flange cross-sectional area. Rehm (1987) also found large-scale reduction in cross-sectional area (over 30%) only produced small and less detectable shifts in the modal frequency (less than 1%). Because a shift in modal frequency is a global parameter of the

structure, it provides no clear and precise means of identifying more than damage existence. Damage of the same size but in different locations of the structure may produce the same amount of frequency change. This has led many researchers to investigate the use of more sensitive modal parameters to detect and locate damage.

Formulas and algorithms using displacement mode shapes and curvature mode shapes have been used to better locate the damage. Yuen (1985) in his paper investigated the first five mode shapes of a damaged cantilever beam, varying the location and the degree of damage within the beam. He modeled the crack as a reduction in the modulus of elasticity. He borrowed this procedure of reducing the modulus of elasticity from Adams (1978), who reduced the modulus of elasticity to zero in the damaged area. Yuen (1985) found that a reduction in the modulus of elasticity of 50% produced a small but measurable change in both the first modal frequency and mode shape. He further added that the expected change in vibration amplitude was measurable and would demand the same order of accuracy as the frequency measurement. In this study, he failed to mention the exact order of accuracy required. In a study conducted by Pandey (1994), changes in mode shape curvature were used to identify and locate damage in a simply supported beam and a

cantilever beam model. Pandey (1994) reverted to the common practice of reducing the modulus of elasticity to model the damaged section. However, he showed that damages detected by changes in mode shape curvature were localized to the region of damage while changes in the mode shape displacement were not localized.

The carrying precedence in the majority of articles reviewed was crack damage continuously being modeled as a reduction in the flexural stiffness (EI) of the damaged elements. In almost all cases, there was no considerable effort provided to explain the linearization of dynamic response for neither crack damage nor sufficient evidence to support the amount of material property or geometric property reduction used in the analysis. Following this procedure, there is no clear relationship between the geometrical dimensions of the crack and the amount of reduced flexural stiffness incurred within the structure. This method also provides no exact correlation between the damaged section's effect on the global and local dynamic response of the structure among the different modes of vibration. Therefore, there is a need to clarify the differences between the linearization in dynamic response of embedded local crack damage and the direct representation of embedded local crack damage in a finite element model.

THIS PAGE INTENTIONALLY LEFT BLANK

III. FINITE ELEMENT MODELING AND ANALYSIS

A finite element model was generated using beam elements with displacement degrees of freedom only. The detailed derivation is given by Kwon and Bang (1997) and is therefore omitted in the following sections. As seen in Fig. 1, each element has six degrees of freedom. There are four axial displacement dof's at the corner points and two transverse displacement dof's at the endpoints of the element.

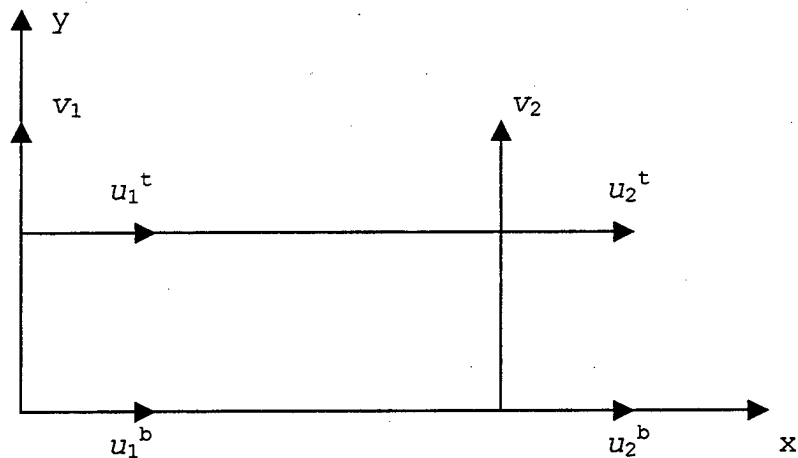


Figure 1. Four-Noded Beam Element with Six Dof's

The displacement field of the element is

$$\{\bar{u}\} = \begin{Bmatrix} u(x, y) \\ v(x) \end{Bmatrix} = [N] \{d^e\} \quad (1)$$

where $[N]$ is the linear shape function matrix and $\{d^e\}$ is the vector of nodal displacements. The axial normal strain can be written as

$$\varepsilon_x = \frac{\partial u}{\partial x} = \frac{\partial N_1}{\partial x} H_1 u_1^b + \frac{\partial N_1}{\partial x} H_2 u_1' + \frac{\partial N_2}{\partial x} H_1 u_2^b + \frac{\partial N_2}{\partial x} H_2 u_1' \quad (2)$$

and the shear strain is

$$\gamma_{xy} = \frac{\partial u}{\partial y} + \frac{\partial v}{\partial x} = \frac{\partial H_1}{\partial y} N_1 u_1^b + \frac{\partial H_2}{\partial y} N_1 u_1' + \frac{\partial H_1}{\partial y} N_2 u_2^b + \frac{\partial H_2}{\partial y} N_2 u_2' + \frac{\partial N_1}{\partial x} v_1 + \frac{\partial N_2}{\partial x} v_2 \quad (3)$$

The element stiffness matrix was obtained by minimizing the total strain energy which contains both bending and transverse shear energy.

$$[K^e] = [K^e]_b + [K^e]_s \quad (4)$$

The subscripts 'b' and 's' indicate bending and transverse shear, respectively. The bending and transverse shear stiffness matrices are

$$[K_b^e] = \int_0^l \int_0^h \{B_b\}^T E \{B_b\} dx dy \quad (5)$$

$$[K_s^e] = \int_0^l \int_0^h \{B_s\}^T E \{B_s\} dx dy \quad (6)$$

where E and G are the elastic and shear modulii of the beam and the vectors $\{B_b\}$ and $\{B_s\}$ are derived from the strain-displacement relationship given below.

$$\varepsilon_x = \{B_b\} \{d^e\} \quad (7)$$

$$\gamma_{xy} = \{B_s\} \{d^e\} \quad (8)$$

By carrying out the integration, the bending and transverse shear stiffness matrices are obtained.

$$[K_b^e] = \frac{Eh}{6l} \begin{bmatrix} 2 & 1 & 0 & -2 & -1 & 0 \\ 1 & 2 & 0 & -1 & -2 & 0 \\ 0 & 0 & 0 & 0 & 0 & 0 \\ -2 & -1 & 0 & 2 & 1 & 0 \\ -1 & -2 & 0 & 1 & 2 & 0 \\ 0 & 0 & 0 & 0 & 0 & 0 \end{bmatrix} \quad (9)$$

and

$$[K_s^e] = \frac{1}{4lh} \begin{bmatrix} Gl^2 & -Gl^2 & 2Glh & Gl^2 & -Gl^2 & -2Glh \\ -Gl^2 & Gl^2 & -2Glh & -Gl^2 & Gl^2 & 2Glh \\ 2Glh & -2Glh & 4Gh^2 & 2Glh & -2Glh & -4Gh^2 \\ Gl^2 & -Gl^2 & 2Glh & Gl^2 & -Gl^2 & -2Glh \\ -Gl^2 & Gl^2 & -2Glh & -Gl^2 & Gl^2 & 2Glh \\ -2Glh & 2Glh & -4Gh^2 & -2Glh & 2Glh & 4Gh^2 \end{bmatrix} \quad (10)$$

The element stiffness matrix, which is obtained by adding the bending and transverse shear stiffness matrices, can be expressed in the following form

$$[K^e] = \begin{bmatrix} (a_1 + 2a_3) & (-a_1 + a_3) & a_4 & (a - 2a) & (-a_1 - a_3) & -a_4 \\ (-a_1 + a_3) & (a_1 + 2a_3) & -a_4 & (-a_1 - a_3) & (a_1 - 2a_3) & a_4 \\ a_4 & -a_4 & a_2 & a_4 & -a_4 & -a_2 \\ (a_1 - 2a_3) & (-a_1 - a_3) & a_4 & (a_1 + 2a_3) & (-a_1 + a_3) & -a_4 \\ (-a_1 - a_3) & (a_1 - 2a_3) & -a_4 & (-a_1 + a_3) & (a_1 + 2a_3) & a_4 \\ -a_4 & a_4 & -a_2 & -a_4 & a_4 & a_2 \end{bmatrix} \quad (11)$$

where each symbol denotes

$$a_1 = \frac{Gl}{4h} \quad a_2 = \frac{Gh}{l} \quad a_3 = \frac{Eh}{6l} \quad a_4 = \frac{G}{2}$$

In the mass matrix, a lumped mass was used where the mass was concentrated at the six nodal degrees of freedom.

$$[M^e] = \frac{\rho h l b}{4} \begin{bmatrix} 1 & 0 & 0 & 0 & 0 & 0 \\ 0 & 1 & 0 & 0 & 0 & 0 \\ 0 & 0 & 2 & 0 & 0 & 0 \\ 0 & 0 & 0 & 1 & 0 & 0 \\ 0 & 0 & 0 & 0 & 1 & 0 \\ 0 & 0 & 0 & 0 & 0 & 2 \end{bmatrix} \quad (12)$$

The $\rho h l b$ term is the element mass and is distributed among the four axial displacement dof's and two transverse displacement dof's.

Once the system mass and stiffness matrices are computed for the beam, they are substituted into the equation of motion of an undamped vibrating system.

$$[M]\{\ddot{x}\} + [K]\{x\} = 0 \quad (13)$$

After applying the proper boundary conditions, the above equation is solved using the eigenvalue equation given below.

$$([K] - \lambda_i^2 [M])\Phi_i = 0 \quad (14)$$

The term λ_i represents the modal frequencies and Φ_i represents the vector of corresponding displacement mode shapes.

Although damage can be detected from the change in displacement mode shapes, finding the location of the damage is very difficult. Pandey (1994) found that changes in displacement mode shapes are not localized to damage areas. Therefore, other parameters which are more sensitive to the location of the damage must be utilized. Mode shape curvature is related to the flexural stiffness of a beam cross-section by the following relationship:

$$\Phi'' = \frac{M}{EI} \quad (15)$$

where Φ'' is the curvature at the section, M is the Bending moment, and EI is the flexural stiffness. From the displacement mode shapes, curvature mode shapes were obtained numerically by using a weighted central difference approximation.

$$\Phi'' = 2 \left(\frac{\Phi_{j+1}(x_j - x_{j-1}) - \Phi_j(x_{j+1} - x_{j-1}) + \Phi_{j-1}(x_{j+1} - x_j)}{(x_j - x_{j-1})(x_{j+1} - x_{j-1})(x_{j+1} - x_j)} \right) \quad (16)$$

Pandey (1994) successfully showed the benefits of using mode shape curvature to detect and locate damage in simply supported and cantilever beam, where damage was simulated by a 50% reduction in the modulus of elasticity.

IV. FINITE ELEMENT MODEL COMPARISON

A. MODEL

The material properties for an aluminum alloy (1100-H14) were used to generate a mesh for a 48cm x 2.54cm x 1.27cm beam. The beam was modeled as a single row of eighty elements with the majority of elements concentrated around the damaged section. A 2.4 cm, through the width, axial crack located at the midpoint of the beam was simulated by reducing the modulus of elasticity in the elements of the damaged section. Another beam was generated, having two rows of eighty elements with the majority of elements concentrated around the damaged section. A total of 160 spaced elements were used for this model. Transverse displacement degrees of freedom were coupled along the beam axis. Axial displacement continuity was enforced along the interface of the top and bottom row of elements. An embedded, through the thickness, crack was simulated by uncoupling the axial and transverse degrees of freedom between the top and bottom row of elements. The finite element models are included in Figs. 2 and 3.

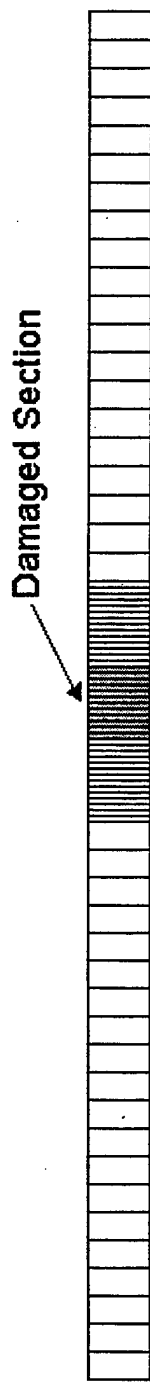


Figure 2. Finite Element Mesh for Beam with Reduced Modulus in Damaged Section

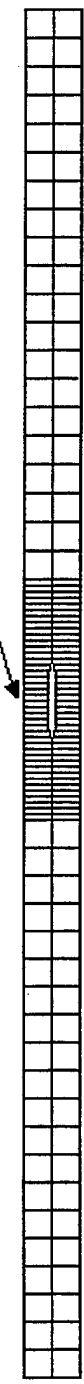


Figure 3. Finite Element Mesh for Beam with Embedded Crack

B. RESULTS

The eigenvalue problem was solved for the finite element model of the undamaged beam and the beam with an embedded crack. The first five non-zero modal frequencies and corresponding mode shapes were obtained for the damaged and undamaged beam using the embedded crack model. Only transverse displacement dof's were considered for the mode shapes. The absolute shift in the modal frequencies due to the presence of the crack was calculated and listed in Table 1. Once the modal frequency shifts were calculated, the modulus of elasticity in the damaged elements of the other finite element model were adjusted until the corresponding modal frequency shifts were approximately equal to those experienced by the finite element model with the embedded crack. Simultaneously matching the first five non-zero modal frequency shifts was impossible. However, by reducing the modulus a very small amount ($7 \times 10^{-7}\%$), the first non-zero modal frequency shift was matched closely as seen in Table 2. As seen in Table 3, reducing the modulus a very large amount (75%) matched the second and the fourth non-zero modal frequency shifts between the embedded crack model and the reduced modulus model.

Table 1. Frequencies for Embedded Crack Model

Mode	Undamaged λ (Hz)	Damaged λ' (Hz)	$ \lambda - \lambda' $ (Hz)
1	28.6688	28.6688	~0
2	78.6241	78.4692	.1549
3	152.8576	152.8549	.0027
4	250.6039	249.1599	1.4440
5	369.9797	369.9429	.0368
			Ave=.3277

Table 2. Frequencies for 7e-7% Reduced Modulus Model

Mode	Undamaged λ (Hz)	Damaged λ' (Hz)	$ \lambda - \lambda' $ (Hz)
1	28.6075	28.6075	~0
2	78.2601	78.2601	~0
3	151.6761	151.6761	~0
4	247.7349	247.7349	~0
5	364.2232	364.2231	.0001
			Ave=~0

Table 3. Frequencies for 25% Reduced Modulus Model

Mode	Undamaged λ (Hz)	Damaged λ' (Hz)	$ \lambda - \lambda' $ (Hz)
1	28.6075	24.3586	4.2490
2	78.2601	78.1053	0.1548
3	151.6761	137.7113	13.9648
4	247.7349	246.2816	1.4534
5	364.2232	336.8181	27.4050
			Ave=9.4454

An average of the first five modal frequencies was calculated for the embedded crack model and corresponded to the average frequency change of a model with a 6% decrease

in the modulus of elasticity in the damaged section. The values for the modal frequencies are listed below in Table 4. Although the average change in the first five non-zero modal frequencies matched the average change of the embedded crack model, the individual changes in modal frequency nor their corresponding changes in displacement mode shapes matched the changes experienced by the embedded crack model.

Table 4. Frequencies for 94% reduced Modulus Model

Mode	Undamaged λ (Hz)	Damaged λ' (Hz)	$ \lambda - \lambda' $ (Hz)
1	28.6075	28.4938	.1137
2	78.2601	78.2568	.0033
3	151.6761	151.2246	.4515
4	247.7349	247.7042	.0307
5	364.2232	336.1971	1.0261
			Ave=.3251

Although the modal frequency shifts caused by the crack presence could be matched separately, matching their corresponding changes in the displacement mode shapes was rather difficult. Even numbered displacement mode shapes matched with close accuracy when matching their corresponding change in modal frequency. However, the displacement mode shape changes for the first mode shape and all other odd numbered modes shapes could not be matched to the changes experienced by the embedded crack model by any alteration of the modulus of elasticity in the damaged section. Altering the modulus of elasticity in the damaged

section had a more global effect on the change in the odd numbered displacement mode shapes than the embedded crack model for the given damage scenario. The magnitude of displacement change in the reduced section modulus model was also found to be significantly lower than the displacement change found in the embedded crack model when the first modal frequency change was matched. It was very clear that there existed some difference between the models that could not be corrected by any justifiable alteration in the modulus of elasticity in the damaged section.

V. LINEAR DYNAMIC ANALYSIS

A. MODEL

The same material properties for the aluminum alloy (1100-H14) beam used in the comparison of reduced material property damage and the embedded crack damage models were used to generate the mesh for the first study in the Linear Dynamic Analysis. Having acknowledged the differences between the dynamic response of an embedded crack model and a reduced modulus of elasticity model, the modal frequencies, mode shape displacements, and mode shape curvatures were calculated for a free-free beam with and without a 2.4 cm embedded crack using the embedded crack model. Each modal parameter was compared for sensitivity to damage detection and localization.

The analysis was further carried out on a finite element mesh representation of a sandwiched composite beam with the following dimensions 48 cm x 4 cm x .8 cm. In the finite element model, Syntac 350C foam of .6 cm thickness (Young's Modulus= 2.21×10^5 N/cm² Poisson's Ratio=.35, Density= 9.61×10^{-5} kg/cm³, Modulus of Rigidity= 8.18×10^4 N/cm²) was reinforced by two .1 cm thick layers of Glass Reinforced Plastic (Young's Modulus= 2.07×10^6 N/cm²

Poisson's Ratio=.342, Density= 3.06×10^{-3} kg/cm³, Modulus of Rigidity= 8.97×10^5 N/cm²). The finite element model of the composite beam is included in Fig. 4. The laminae were modeled as perfectly joined at the interface except in the damaged section, where delamination was simulated. The size of the crack was varied between 2.4 cm and 3.6 cm. The location of the crack was also varied between the beam midpoint and 10 cm away from the midpoint. Three separate boundary conditions were applied to the model. (Free-Free, Simply Supported, and Cantilever)

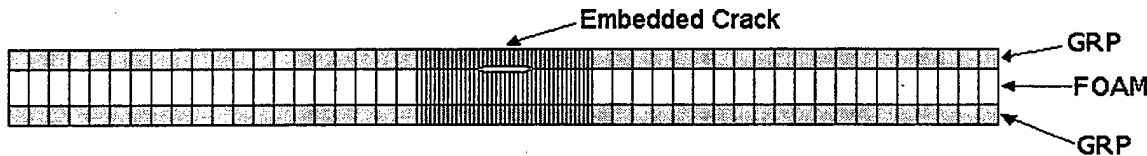


Figure 4. Finite Element Mesh for Composite Beam with Crack

B. RESULTS

The data collected from the embedded crack model was used to detect and locate the embedded, through the thickness, crack. The maximum values of percent relative change for each curvature mode shape and displacement mode shape as well as the percent relative change in modal frequency are listed below in Table 5. As previously mentioned, the modal frequencies are almost insensitive to the embedded crack damage. It was also hard to derive the

location of the crack from the modal frequency shift due the possibility of different cracks producing the same shift in modal frequency. Therefore, the analysis was more focused on the mode shape displacement and mode shape curvature values. In all modes, the maximum values of relative change were higher for curvature mode shapes, displaying a higher sensitivity to the presence of damage.

Table 5. Maximum Percent Change

Mode	Percent $\Delta\lambda$	Maximum percent $\Delta\phi$	Max. percent $\Delta\phi''$
1	~0	0.0006	0.5912
2	0.1970	5.4413	297
3	0.0018	0.2879	4.2053
4	0.5762	15.241	291
5	0.0099	0.3151	10.228

Plots of the displacement and curvature mode shapes are included in Figs. 5 through 14. As seen in the figures, changes in curvature mode shapes were more localized to the region of damage than changes in displacement mode shapes.

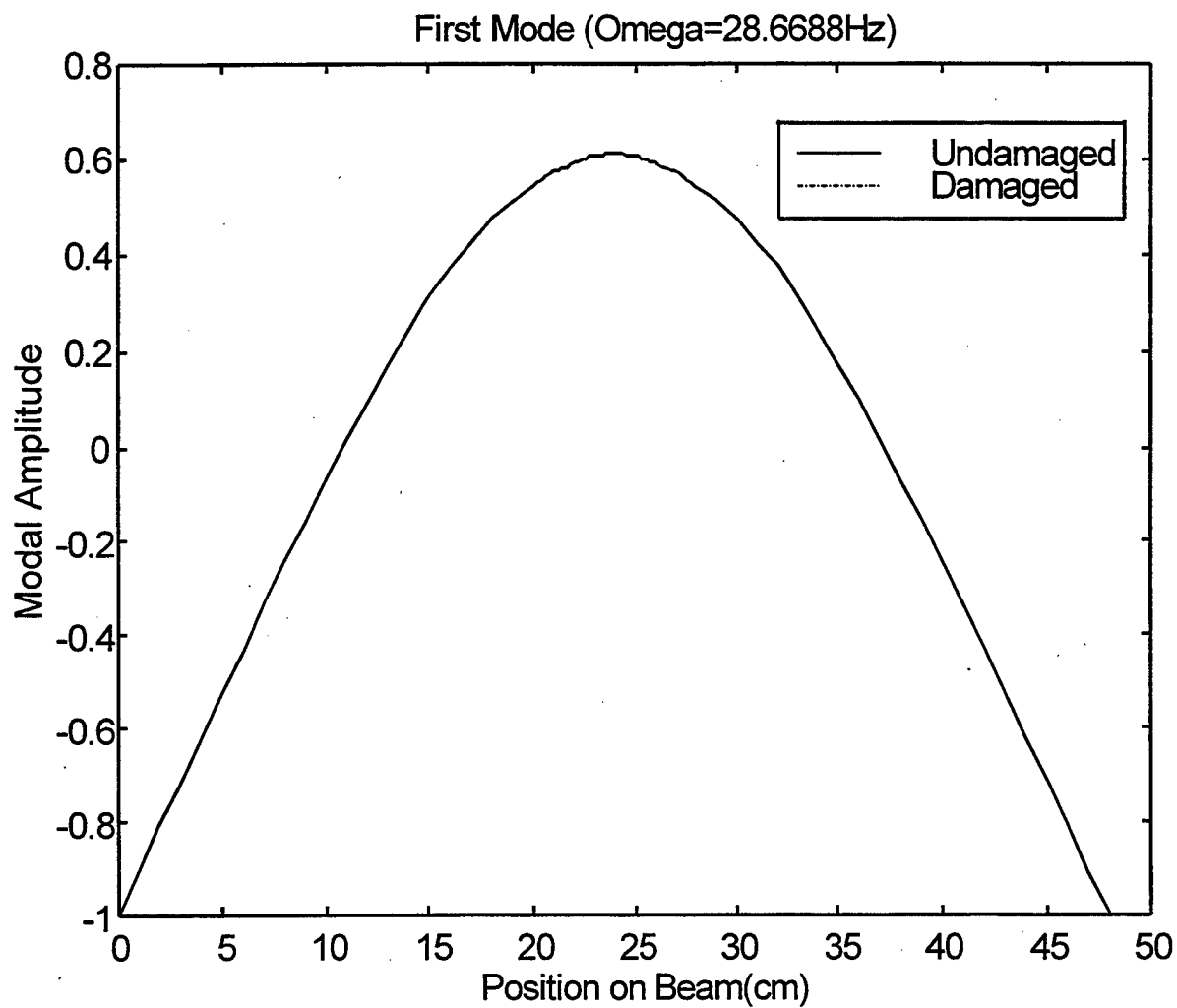


Figure 5. First Modal Displacement of Embedded Crack Model

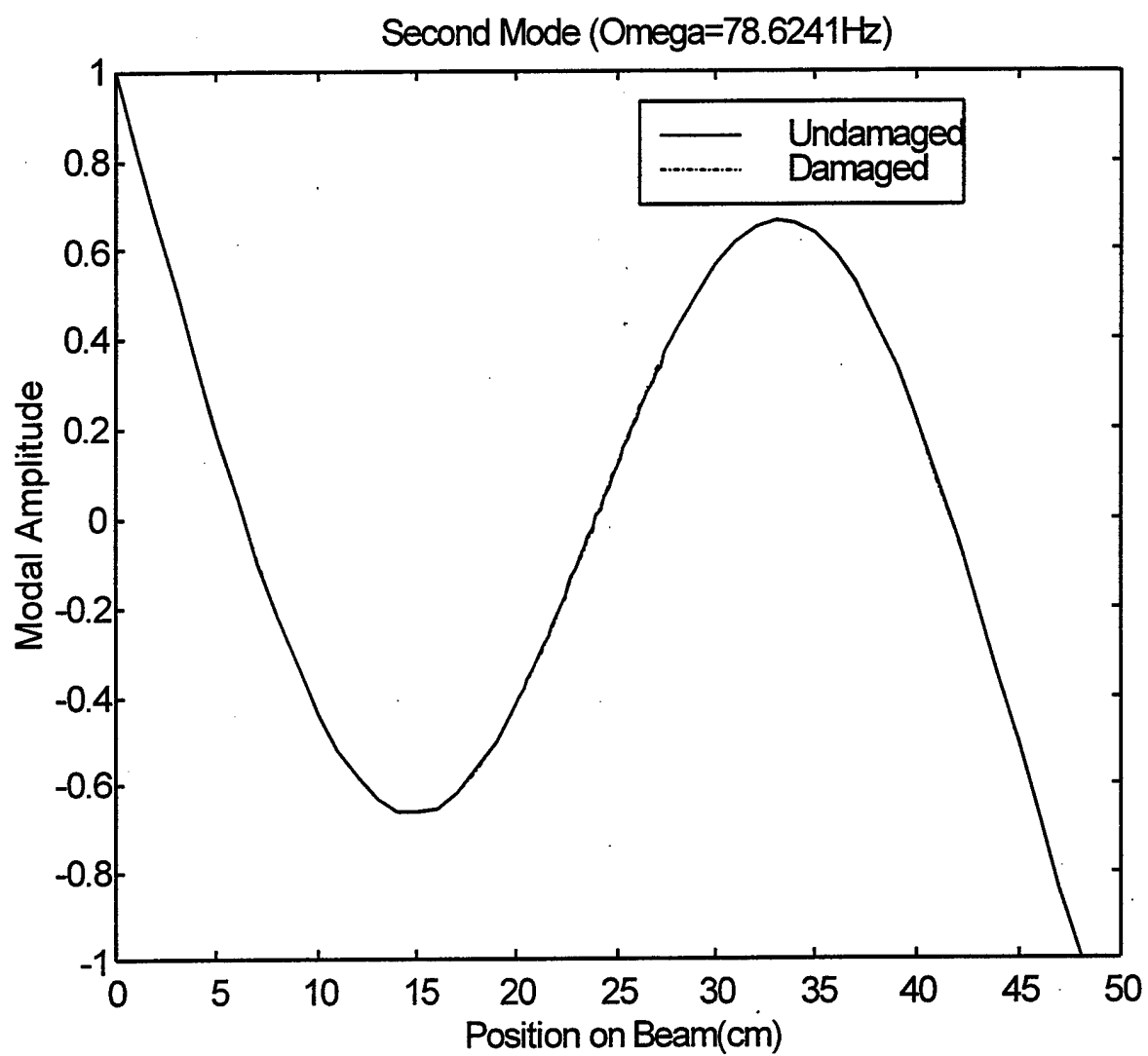


Figure 6. Second Modal Displacement of Embedded Crack Model

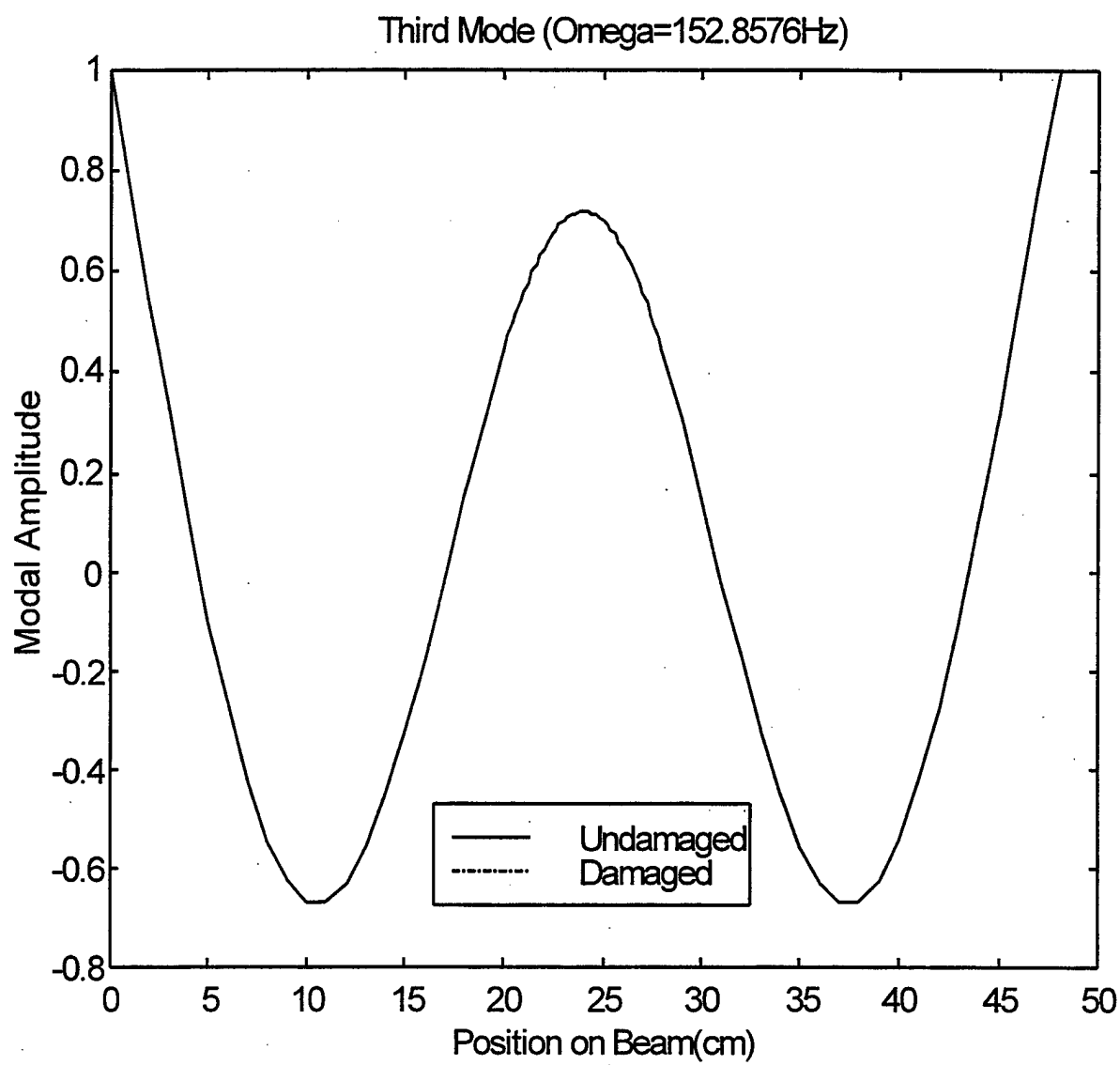


Figure 7. Third Modal Displacement of Embedded Crack Model

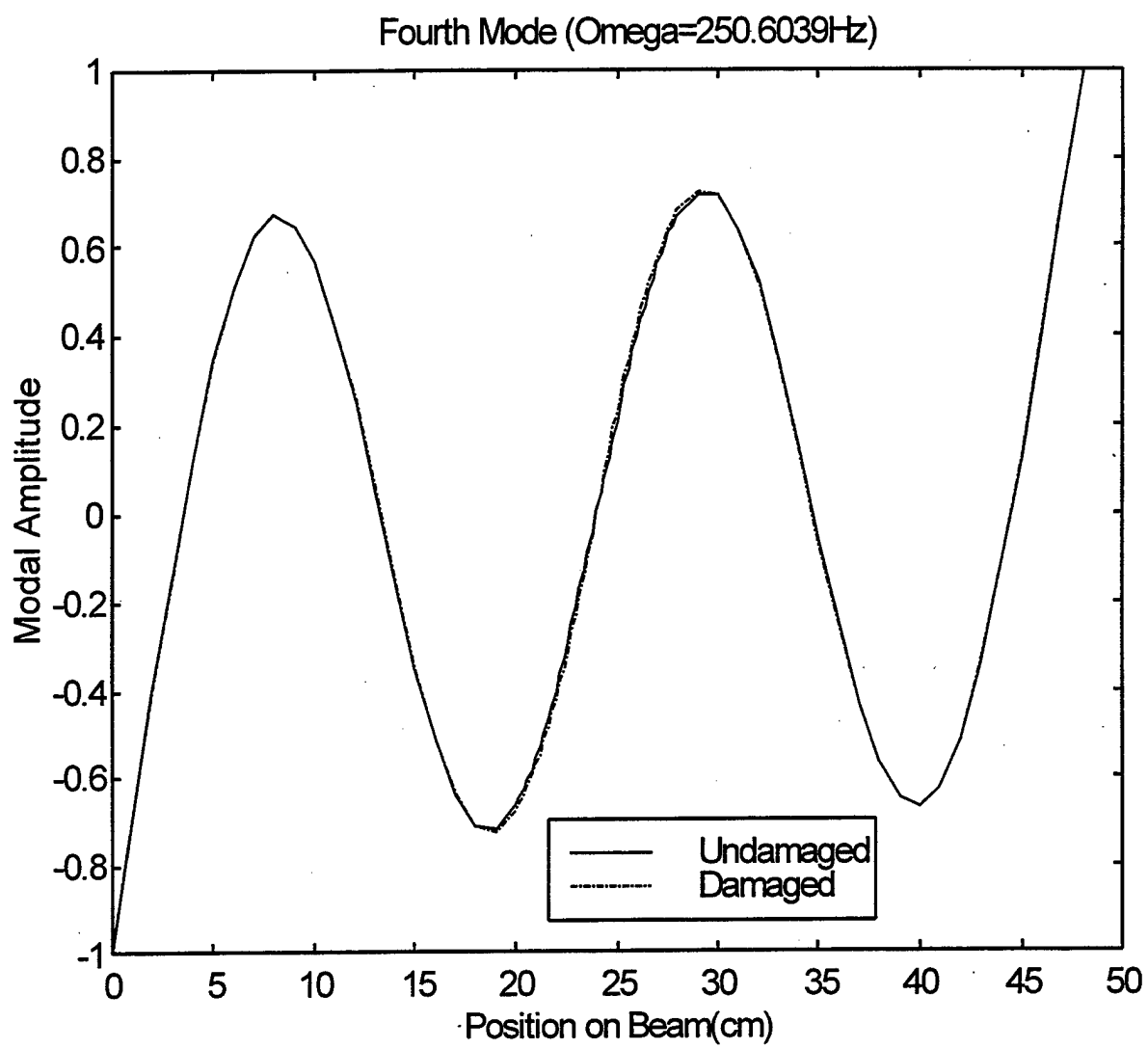


Figure 8. Fourth Modal Displacement of Embedded Crack Model

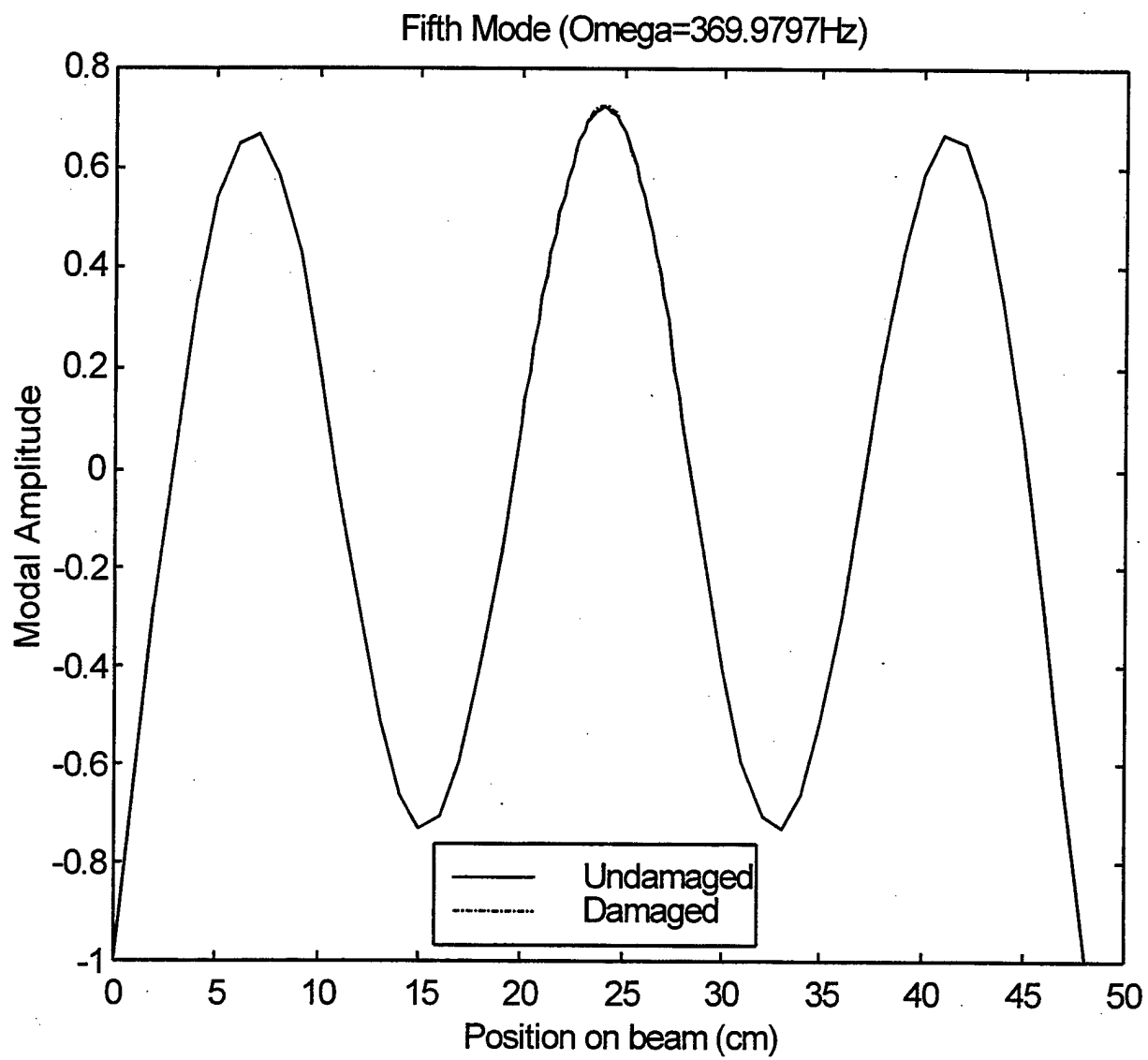


Figure 9. Fifth Modal Displacement of Embedded Crack Model

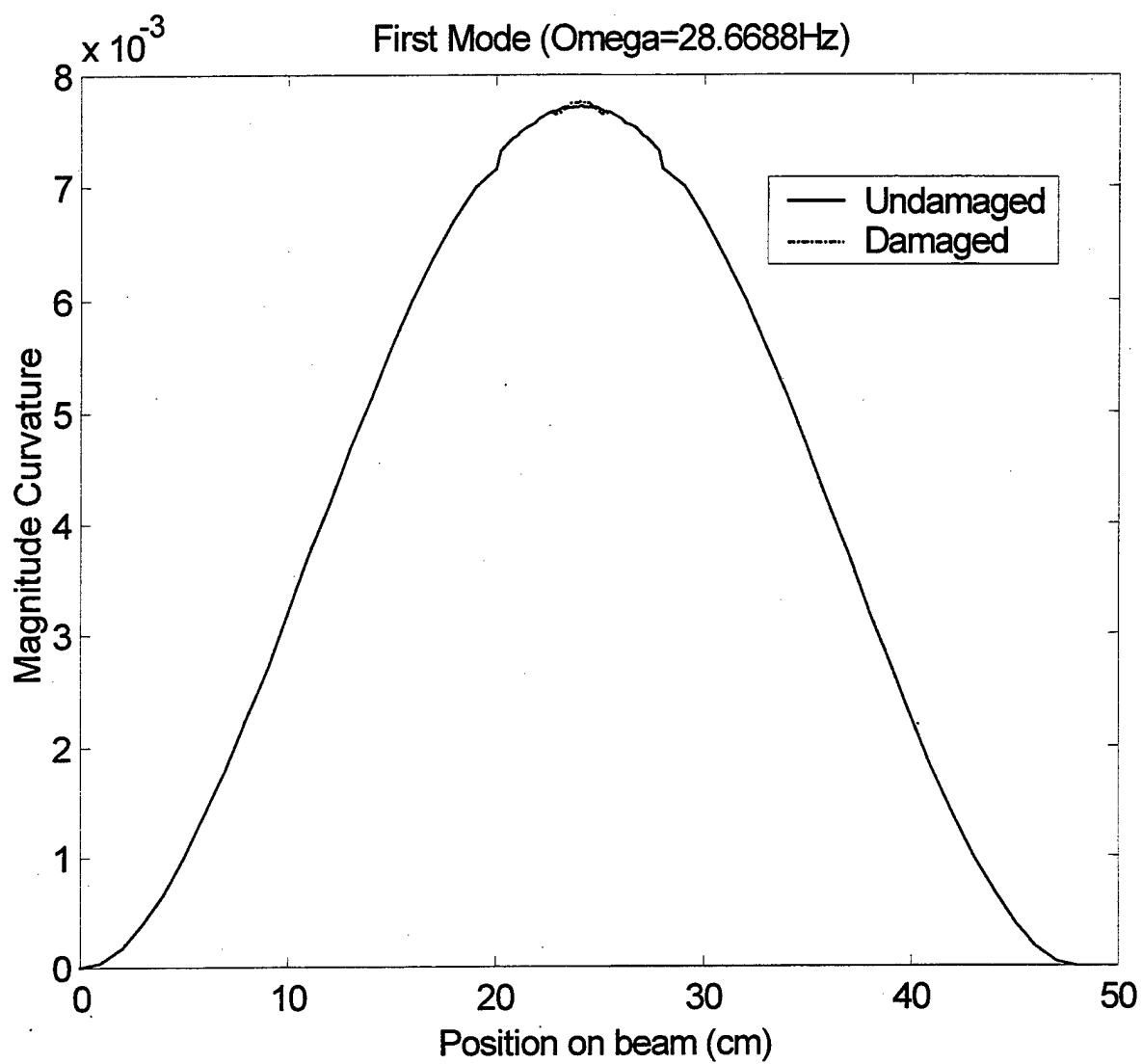


Figure 10. First Curvature Mode of Embedded Crack Model

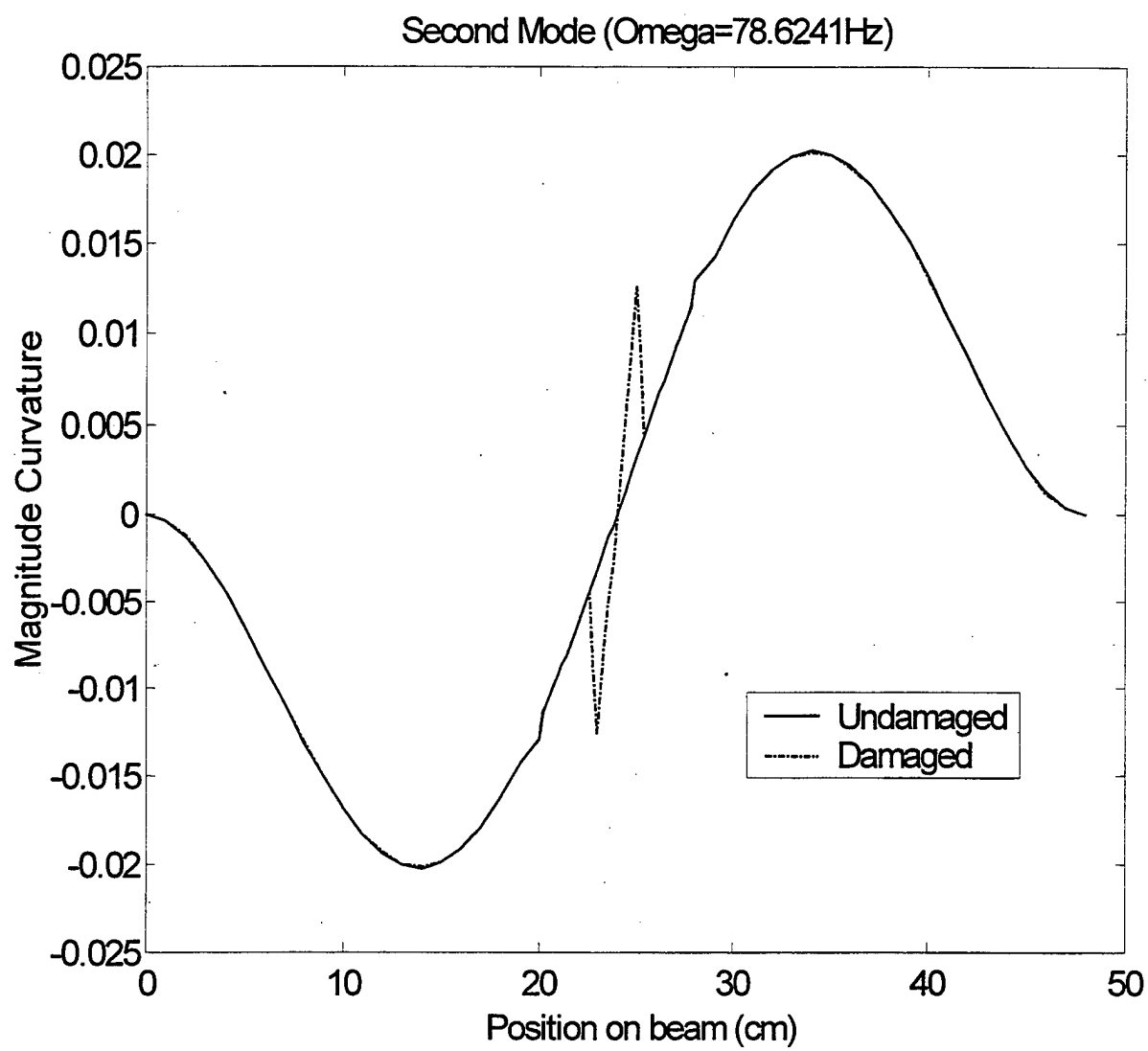


Figure 11. Second Curvature Mode of Embedded Crack Model

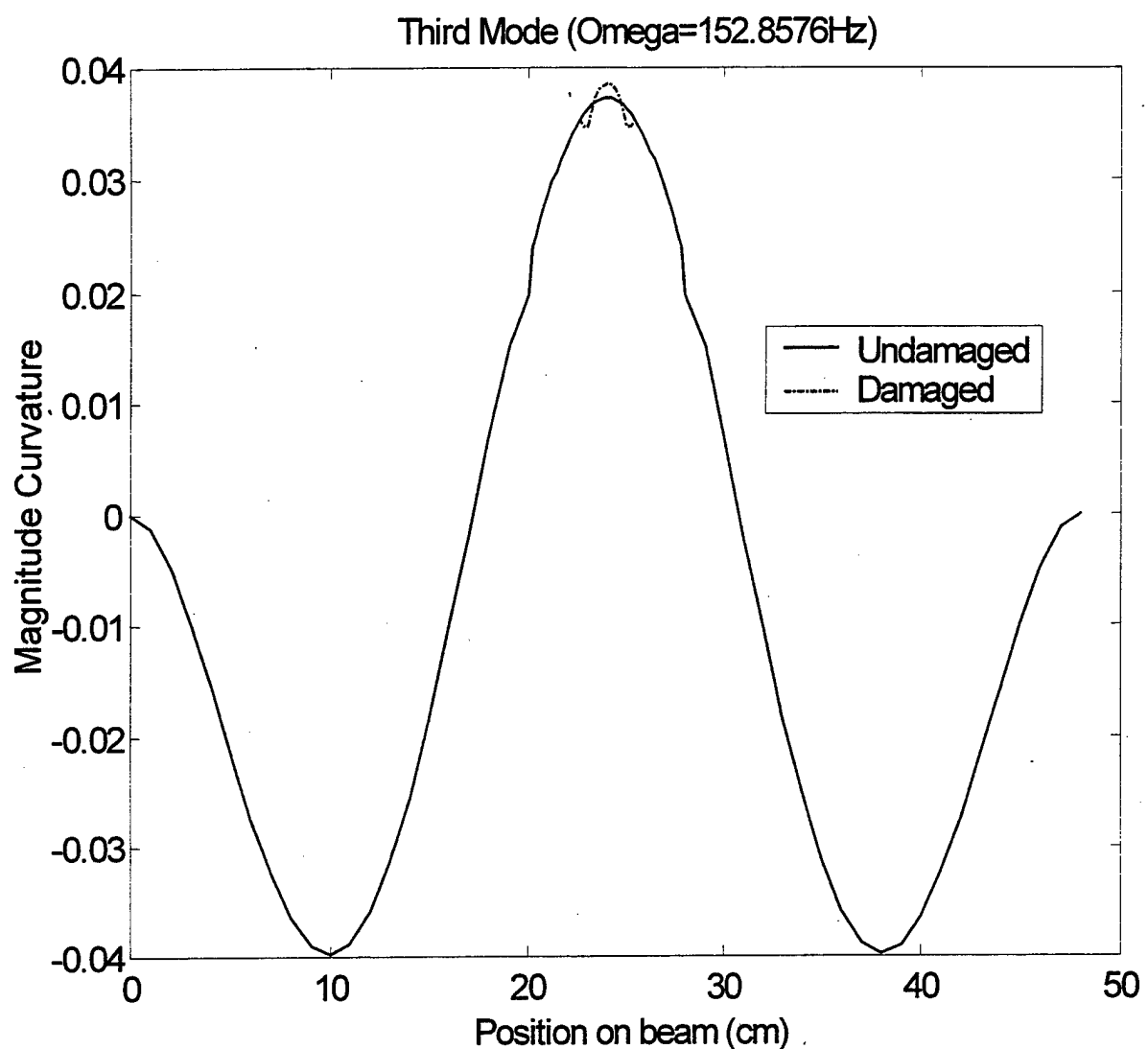


Figure 12. Third Curvature Mode of Embedded Crack Model

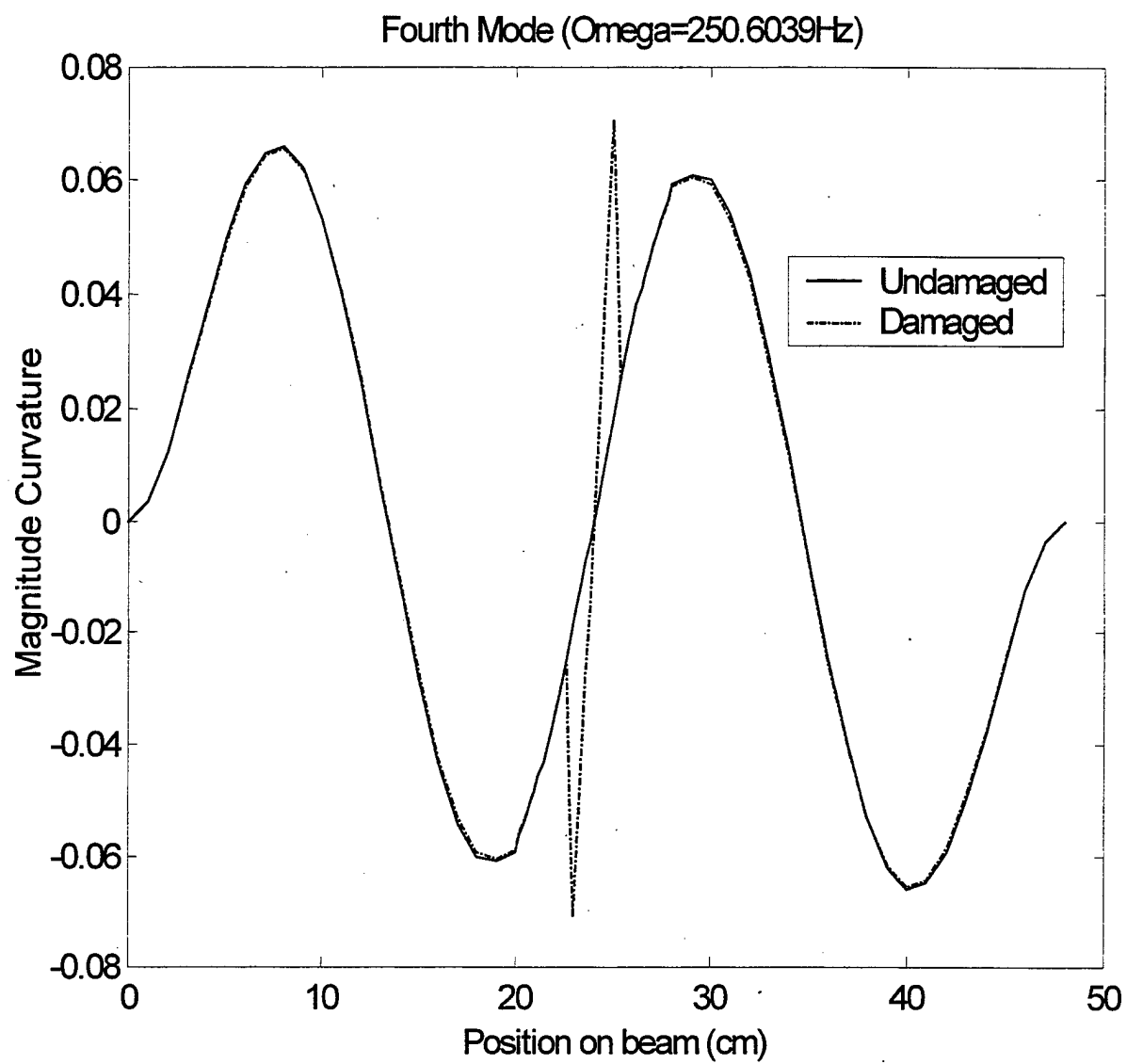


Figure 13. Fourth Curvature Mode of Embedded Crack Model

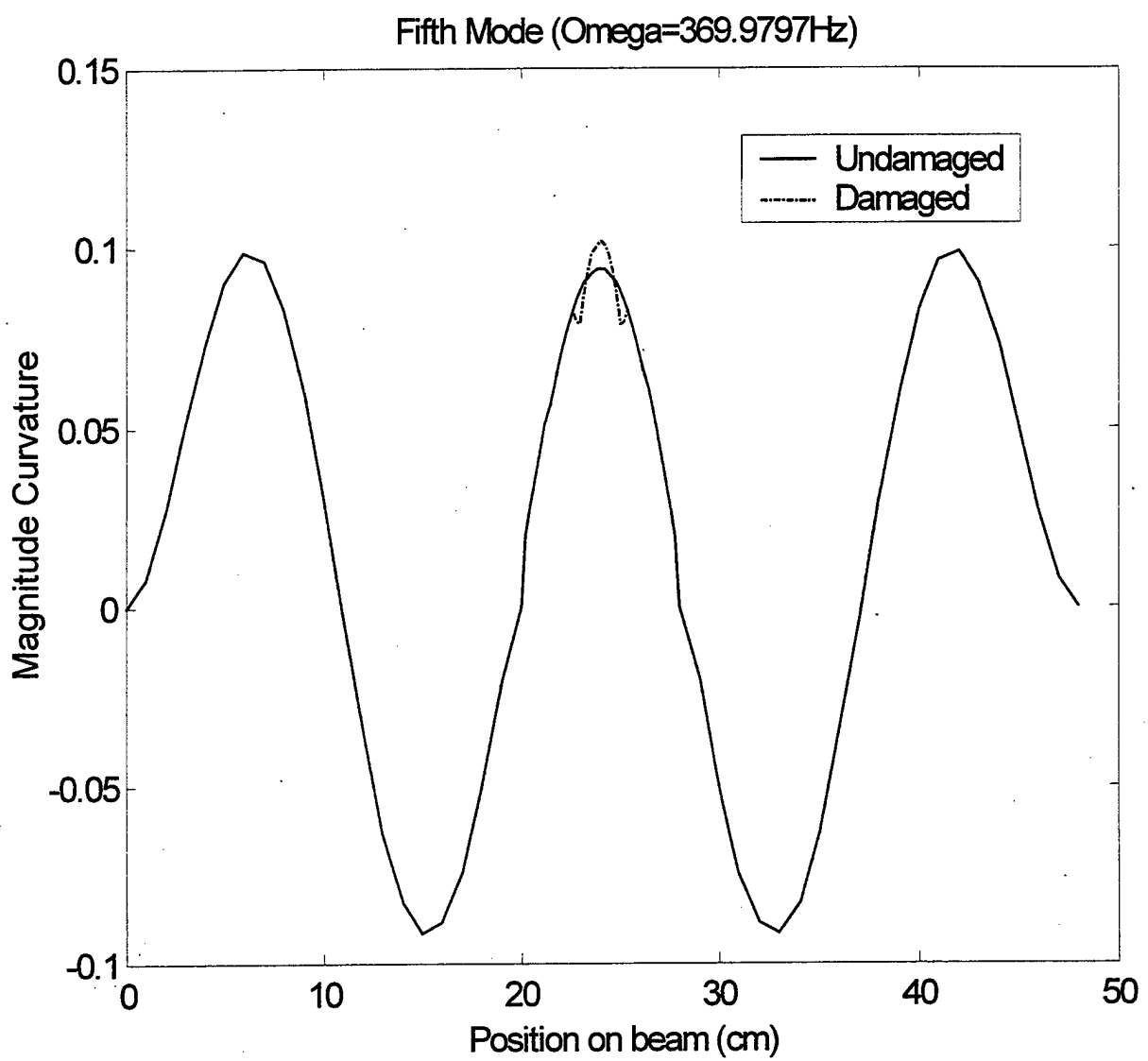


Figure 14. Fifth Curvature Mode of Embedded Crack Model

Modal response data was collected for three different boundary conditions with the size and location of the crack varied. The mode shape changes and mode shape curvature changes were evaluated for each case with hopes of solidifying the change in modal response in terms of crack size, location, and boundary condition.

It was found that the boundary condition applied had a less significant effect on the modal response change generated by an embedded crack of a fixed size and location. This can be attributed to the fact that the odd numbered modes of vibration for a cantilever beam are similar to those of a free/free beam due to symmetry and the response of a simply supported beam is very similar to the response of a free/free beam.

Increasing the crack size increased the amount of change in the modal response, whether considering frequency, mode shape displacement, or mode shape curvature. However, there was not a direct proportional relationship that could be established between the crack size and the amount of change experienced. The change experienced by each mode was significantly different for each case of damage.

The location of the crack in a given mode of vibration affected the amount of crack opening and closure (nonlinear effect) experienced in the response which relates to the

detectability of damage from changes in the modal response. From varying the location of the crack, it was found that the local nature of the crack's effect on modal response became more significant in modes where the reduced stiffness was more evident through crack opening. These locations were around the anti-nodal locations of the mode of vibration. A plot of the more sensitive and less sensitive crack locations is provided below in Figure 15.

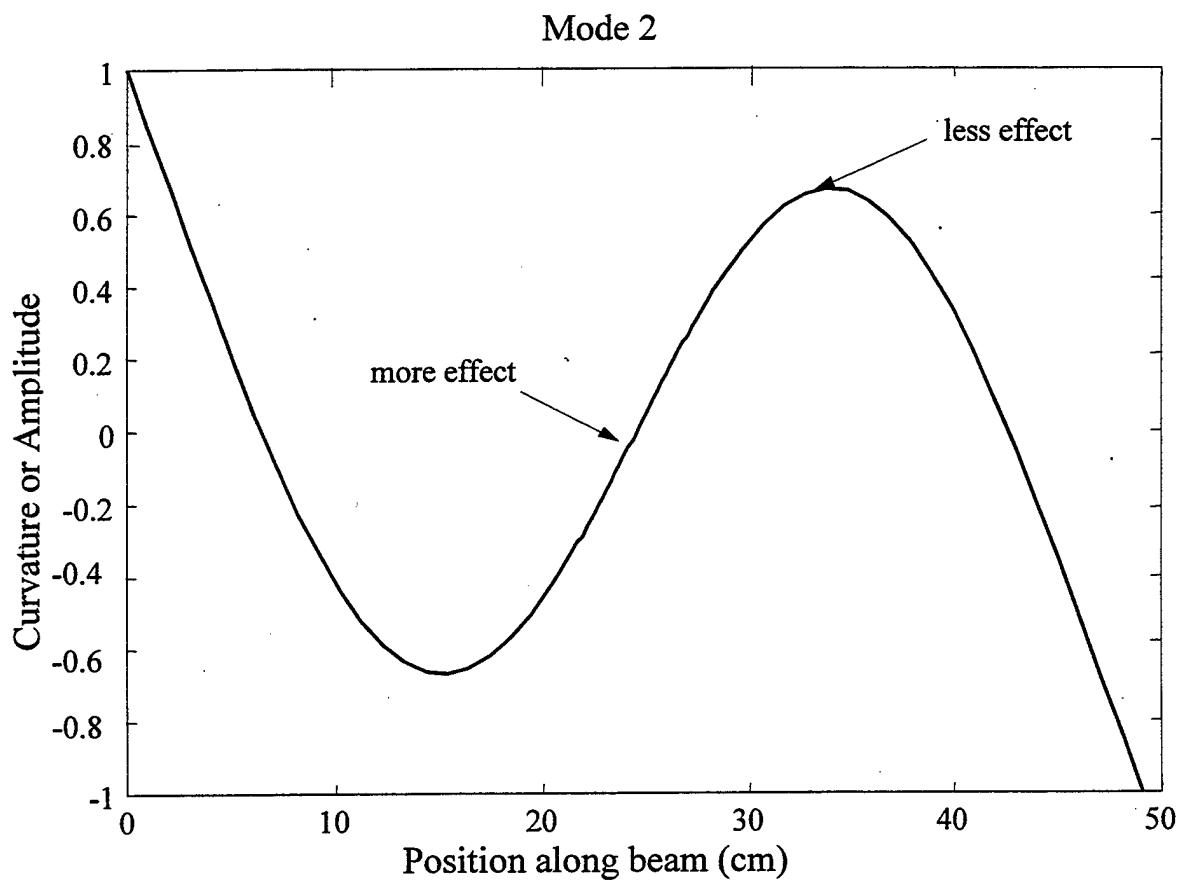


Figure 15. Modal Sensitivity to Damage Plot

THIS PAGE INTENTIONALLY LEFT BLANK

VI. NONLINEAR DYNAMIC ANALYSIS

A. INTRODUCTION

The preceding analysis has concentrated on the linearized effects of crack damage through the use of the eigenvalue problem. The Finite Element mesh generated thus far did not account for contact between the interior surfaces of the crack during a dynamic response. The data collected therefore considers the problem of modal parameter changes due to the effects of crack damage in terms of a stiffness reduction in the location of the crack only. Therefore, an analysis of the transient response of a damaged beam with consideration for the contact surfaces is studied for capturing both the effects of crack surfaces impacting and the nonlinear opening and closure of the crack on the change in dynamic response.

B. ANALYSIS AND RESULTS

To this end, LS-DYNA software was incorporated for the analysis of the nonlinear transient response. A mesh with elements of equal length was generated for the same dimension composite beam used in the Linear Analysis portion

of the current research. Cantilever boundary conditions were applied to the beam which is depicted below in Figure 16.

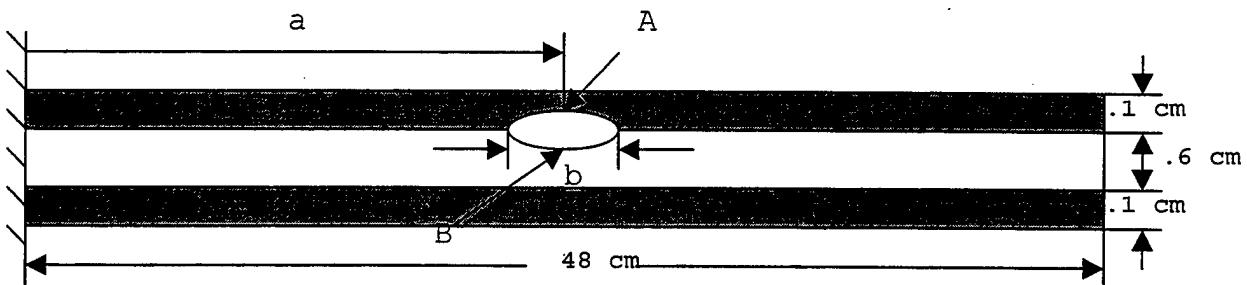


Figure 16. Transient Analysis Model

The location and size of the crack, respectively labeled 'a' and 'b' in the figure above, were varied for the analysis. Natural Frequency values for the first mode of vibration were very close to the values obtained in the linearized analysis. Frictional impact surfaces were created between the surfaces of the crack. The friction coefficient was varied to evaluate the amount of frictional dissipation of energy involved with crack vibration during a transient response. Since the exact value for the friction coefficient for a crack surface was unknown, values were chosen in an effort to relate the lack of smoothness that would be found on the crack surface. The embedded crack produces an increase in damping which can be captured by a decrease in successive amplitudes during the transient response of the beam. The following logarithmic decrement equation was used to

calculate the damping ratio values for two consecutive cycles in tip deflection of the beam,

$$\zeta = \frac{\ln\left(\frac{x_1}{x_2}\right)}{\sqrt{\left(\ln\left(\frac{x_1}{x_2}\right) + 4\pi^2\right)}} \quad (17)$$

where ζ is the damping ratio and x_1 and x_2 are successive amplitudes. The results from varying the friction coefficient are included below in Table 6.

Table 6. Damping Ratio According to Friction Coefficient

Friction Coefficient (μ)	Damping ratio
0	~0.000
1	0.0222
2	0.0383

Note: $a=24$ cm, $b=2.4$ cm

The data shows a nonlinear relationship between the friction coefficient and the amount of damping present in the response of a composite beam with a 2.4 cm crack embedded at the midpoint of the beam length. The results from increasing the crack size are included in Table 7.

Table 7. Damping Ratio According to Crack Size

Crack Size 'b' (cm)	Damping Ratio
2.4	0.0222
4.0	0.0281

Note: $\mu=1, a=24$ cm

As observed in the preceding table, there was a 21% increase in modal damping caused by a 40% increase crack size. The effect of crack location on modal damping is summarized in Table 8.

Table 8. Damping Ratio According to Crack Location

Crack Location 'a' (cm)	Damping Ratio
14	0.0153
24	0.0222
34	0.0585

Note: $\mu=1$, $b=2.4$ cm

Important to the analysis was the nonlinear opening and closing of the embedded crack. By plotting the relative axial and transverse displacements of two nodes in direct contact at the midpoint of the crack surface, a clearer picture can be drawn about the periods of contact between the crack surfaces and the amount of nonlinear dissipation of energy through crack surface friction involved when the crack surfaces are in contact. The axial and transverse displacement plots of two nodes at the top and bottom of the crack surfaces (see nodes A and B in Figure 10) during the transient response of a composite beam with a 4.0 cm crack embedded crack at the midpoint of the beam length are provided in Figures 17 and 18.

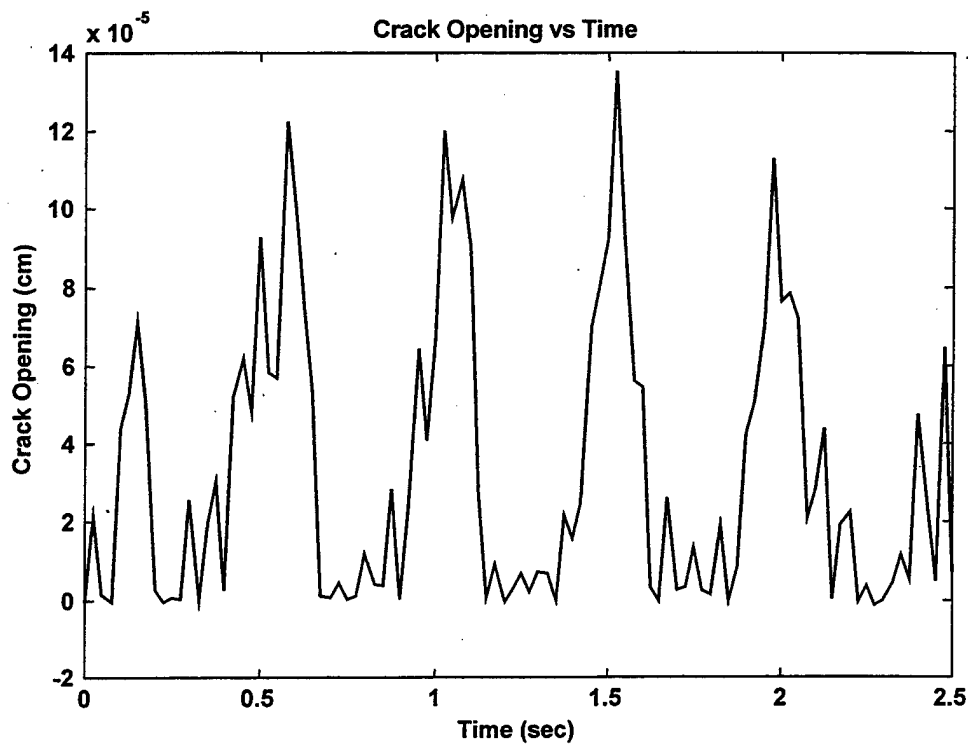


Figure 17. Crack Opening vs Time

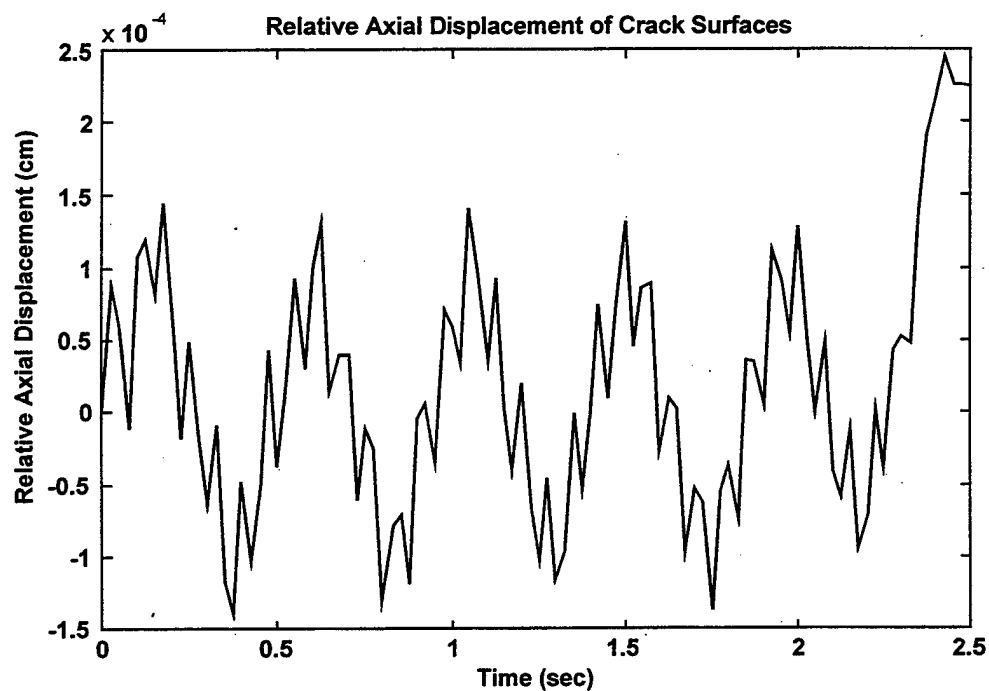


Figure 18. Relative Axial Displacement of Crack Surface

In order for the friction surface of a crack to dissipate energy, there must be both contact and relative motion between the surfaces of the crack. From the plots, it can be seen that contact is only experienced during short time intervals, the relative axial motion during contact is small, and the amount of crack surface separation is also very small. Therefore, the damping ratio obtained through the logarithmic decrement equation is an averaged value of the nonlinear dissipation of energy experienced by the beam. Also, as the crack is placed further away from the cantilever wall, the amount of relative crack surface motion increases thereby causing more damping to occur. This explains the increase in damping ratio in the values of Table 8.

VII. CONCLUSIONS AND RECOMMENDATION

The numerical results of the embedded crack finite element model demonstrate the usefulness of the modeling technique in characterizing the dynamic response of a beam with interior through the thickness crack damage.

Through the direct comparison of the different finite element model dynamic responses, it was shown that there was no concrete correlation between the amount of reduction in the flexural stiffness used in previous research and the response of an embedded crack finite element model. It was also found that the change in modal frequency experienced by the embedded crack model was quite small and was only comparable to a smaller reduced stiffness model vice the 30-50% reduction used in previous research. Furthermore, mode shape curvature was a more sensitive indicator of damage and a better locator of damage than modal frequency or mode shape displacement. The direct approach in modeling an embedded crack was more accurate in capturing the true changes in dynamic response for the different modes of vibration.

From the sandwich composite model analysis, it was shown that boundary conditions have a less significant

effect on the ability to detect damage from modal response changes. It was also shown that crack size was not directly proportional to the amount of change in modal response for all modes of vibration. However, increasing crack size does increase the change in the modal response. Crack location affects the ability to detect damage in certain modes of vibration. Therefore, evaluating a combination of different modes increases the chances of detecting damage from modal response.

The nonlinear transient analysis furthered the study of damage detection by capturing the nonlinear crack opening, crack closure, and relative crack surface sliding motion during the transient response of a cantilever beam with an embedded crack. The friction environment between the surfaces of an embedded crack dissipates energy proportional to the amount of damping experienced by the beam during the transient response. The change in the amount of damping present can provide a means of detecting crack damage and monitoring the extent of crack damage present within the structure.

Recommendations for further study are as follows: investigate higher modes of vibration using the transient nonlinear analysis and frictional dissipation of energy, model multiple embedded cracks of various sizes and

locations, conduct experimentation with both homogenous and composite beams with physical damage and compare to results generate by numerical methods.

THIS PAGE INTENTIONALLY LEFT BLANK

LIST OF REFERENCES

Adams, R.D., Cawley, P., Pye, C.J., and Stone B.J., 1978, "A Vibration Technique for Non-Destructively Assessing the Integrity of Structures," *Journal of Mechanical Engineering Sciences*, **20**, 93-100.

Kwon, Y. W. and Bang, H.C., 1997, *The Finite Element Method Using MATLAB*. CRC Press, Boca Raton, FL.

Pandey, A.K. and Biswas, M., 1994, "Damage Detection in Structures Using Changes in Flexibility," *Journal of Sound and Vibration*, **169**(1), 3-17.

Petro, Samer H., Chen, Shen-En, GangaRao, Hota V.S., and Venkatappa, Suhas, 1997, "Damage Detection Using Vibration Measurements," *Proc. of the 15th International Modal Analysis Conference*, Society of Experimental Mechanics, **1**, 113-119.

Rehm, G., 1987, "Nondestructive Tests for Early Damage Detection," *Proc. US-European Workshop on Bridge Evaluation, Repair, and Rehabilitation*, St. Remy-Les-Chevreuse.

Spyrakos, C., Chen, H.L., Stephens, J., and Govidara V., 1990, "Evaluating Structural Deterioration Using Dynamic Response Characterization," *Proc. Intelligent Structures*, Elsevier Applied Science, 137-154.

Yuen, M.M.F., 1985, "A Numerical Study of Eigenparameters of a Damaged Cantilever," *Journal of Sound and Vibration*, **103**, 301-310.

THIS PAGE INTENTIONALLY LEFT BLANK

BIBLIOGRAPHY

Bernasconi, Dr. O. and Ewins, Prof. D.J., "Application of Strain Modal Testing to Real Structures," *Proc. of the 7th International Modal Analysis Conference*, Society of Experimental Mechanics, 1453-1464.

Ceravola, R. and De Stefano, A., 1995, "Damage Location in Structures Through a Connectivity Use of FEM Modal Analyses," *Modal Analysis: The International Journal of Analytical and Experimental Modal Analysis*, Politecnico di Torino, **10**, 178-186.

Crespo, C., Ruotolo, C., and Surace, C., 1996, "Non-Linear Modeling of a Cracked Beam," *Proceedings of the 14th International Modal Analysis Conference*, Society of Experimental Mechanics, 1017-1022.

Debao', L., Hongcheng, Z., and Bo, Wang, 1989, "The Principles and Techniques of Experimental Strain Modal Analysis," *Proc. of the 7th International Modal Analysis Conference*, Society of Experimental Mechanics, 1285-1289.

Dong, C., Zhang, P.Q., Feng, W.Q., and Hang, T.C., 1994, "The Sensitivity Study of the Modal Parameters of a Cracked Beam," *Proc. of the 7th International Modal Analysis Conference*, Society of Experimental Mechanics, 98-104.

Gudmundson, P., 1982, "Eigenfrequency Changes of Structures Due to Cracks," *Journal of the Mechanics and Physics of Solids*, **30**(5), 339-353.

Kam, T.Y. and Lee, T.Y., 1992, "Detection of Cracks in Structures Using Modal Test Data," *Engineering Fracture Mechanics*, **42**(2), 381-387.

Lindner, D.K., and Kirby, G., 1994, "Location and Estimation of Damage in a Beam Using Identification Algorithms," *Proceedings of 35th AIAA/ASME/ASCE/AHS/ASC Structures, Structural Dynamics and Materials Conference*, 192-198, AIAA-94-1755-CP.

Paolozzi, A. and Peroni, I., 1990, "Detection of Debonding Damage in a Composite Plate Through Natural Frequency Variations," *Journal of Reinforced Plastics and Composites*, **9**, 369-389.

Rizos, P.F., Aspragathos, N. and Dimarogonas, A.D., 1990, "Identification of Crack Location and Magnitude in a Cantilever Beam from the Vibrational Modes," *Journal of Sound and Vibration*, Academic Press Limited, **138**(3), 381-388.

Tsang, W.F., 1990, "Use of Dynamic Strain Measurements for the Modeling of Structures," *Proceedings of the 8th International Modal Analysis Conference*, Society of Experimental Mechanics, 1246-1251.

INITIAL DISTRIBUTION LIST

1. Defense Technical Information Center 2
8725 John J. Kingman Rd., STE 0944
Ft. Belvoir, Virginia 22060-6218
2. Dudley Knox Library 2
Naval Postgraduate School
411 Dyer Rd.
Monterey, California 93943
3. Professor Young W. Kwon, Code ME/Kw 2
Naval Postgraduate School
Monterey, California 93943
4. LT Stephen A. Lipsey, USN 3
4 Indigo Court
Savannah, Georgia 31406
5. Naval Engineering Curricular Office, Code 34 1
Naval Postgraduate School
Monterey, CA 93943-5000